Photoelectrochemical Behavior of a Molecular Ru-Based Water-Oxidation Catalyst Bound to TiO_2-Protected Si Photoanodes

Roc Matheu,[1,2] Ivan A. Moreno-Hernandez,[3] Xavier Sala,[4] Harry B. Gray,[3,5] Bruce S. Brunschwig,[3] Antoni Llobet,*[1,4] Nathan S. Lewis*[3,5,6]

[1] Institute of Chemical Research of Catalonia (ICIQ), Avinguda Països Catalans 16, 43007 Tarragona, Spain.

[2] Departament de Química Física i Inorgànica, Universitat Rovira i Virgili, Marcel·lí Domingo s/n, 43007 Tarragona, Spain.

[3] Beckman Institute Molecular Materials Resource Center, California Institute of Technology, Pasadena, CA 91125, USA

[4] Departament de Química, Universitat Autònoma de Barcelona, Cerdanyola del Vallès, 08193 Barcelona, Spain

[5] Division of Chemistry and Chemical Engineering, California Institute of Technology, Pasadena, CA 91125, USA

[6] Kavli Nanoscience Institute, California Institute of Technology, Pasadena, CA 91125, USA.

Supporting Information

ABSTRACT: A hybrid photoanode based on a molecular water oxidation precatalyst was prepared from TiO_2-protected n- or p^+-Si coated with multiwalled carbon nanotubes (CNT) and the ruthenium-based water oxidation precatalyst [Ru^{IV}(tda)(py-pyr)$_2$(O)], **1(O)** (tda^{2-} is [2,2′:6′,2′′-terpyridine]-6,6′′-dicarboxylato and py-pir is 4-(pyren-1-yl)-N-(pyridin-4-ylmethyl)butanamide). The Ru complex was immobilized by π-π stacking onto CNTs that had been deposited by drop casting onto Si electrodes coated with 60 nm of amorphous TiO_2 and 20 nm of a layer of sputtered C. At pH = 7 with 3 Sun illumination, the n-Si/TiO_2/C/CNT/[**1**+**1(O)**] electrodes exhibited current densities of 1 mA cm^{-2} at 1.07 V vs NHE. The current density was maintained for > 200 min at a constant potential while intermittently collecting voltammograms that indicated that over half of the Ru was still in molecular form after O_2 evolution.

Sustainable production of solar fuels depends on the oxidation of water to O_2(g) to provide an electron source for the concurrent formation of reduced energy-rich molecules.[1] Over the last decade, the specific activity of transition-metal complexes for evolution of O_2(g) from water has increased by four orders of magnitude[2,3] due to judicious design of the ligand environment[4] together with the spectroscopic and electrochemical characterization of intermediates[2,4,5] and the suppression of decomposition pathways.[6]

Anchoring molecular catalysts onto anodes and photoanodes can modify their reaction pathway and can degrade or even improve the activity of the catalyst. Rapid hole trapping by the catalyst could also improve the stability of the light absorber by competing with corrosion or passivation reactions arising from photogenerated charge-carriers in the valence band of the semiconductor.[7]

Molecular complexes immobilized on conductive electrode surfaces have been shown to provide current densities between 0.015 mA cm^{-2} and 0.5 mA cm^{-2} for several hours of O_2(g) evolution from water.[8,9] The immobilized complexes have shown turnover numbers (TON) of 10^4–10^6, comparable to their performance in the homogeneous phase. In contrast, photoanodes functionalized with molecular catalysts have been limited to current densities of ~ 1 mA cm^{-2} for < 20 min,[10,11] and exhibit a decrease in specific activity compared to their behavior in homogeneous conditions, as evidenced by TONs < 1000. Most photoanode designs are based on dye-sensitized schemes in which a [Ru(bpy)$_3$]$^{2+}$ derivative dye and a molecular water-oxidation catalyst are co-anchored onto the surface of a large band-gap semiconductor. The dyes are responsible for light absorption and electron injection into the semiconductor, while the holes are responsible for catalyst activation that eventually leads to water oxidation. This strategy is generally limited by rapid back electron-transfer processes, dye photodegradation, and desorption of the both the dye and the catalysts.[12,13] Despite these limitations, dye-sensitized photoanodes have been integrated in tandem devices for H_2 evolution by the use of buried Si pn junctions.[11b]

Chart 1. Ligands and complexes employed in this work.

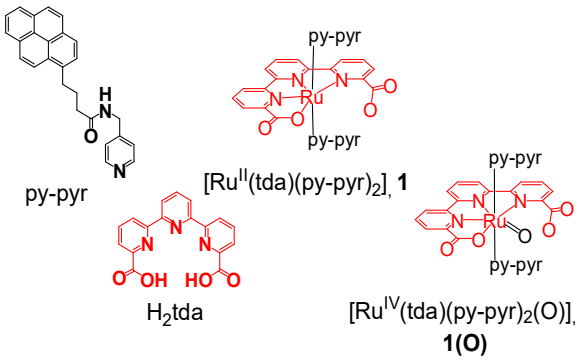

An alternative to dye-sensitized oxide-based photoelectrodes is to couple a water-oxidation catalyst to a small band-gap semiconductor, such as Si, GaAs or GaP that has been protected with a coating based on TiO_2, NiO_x or CoO_x.[14,15] This coating strategy has been shown to produce stable photoanodes that can operate for months under strongly anodic conditions in highly alkaline or near-neutral pH electrolytes.[15]

Scheme 1. Schematic representation of a cross-section of a Si photoanode decorated with the molecular water oxidation precatalyst **1(O)** (red circles). The photoanode contains a 20 nm carbon layer (green) that had been sputtered over a 60 nm TiO_2 layer (orange) previously deposited by ALD over Si (red). CNTs (grey) were deposited over this material by drop casting and then the precatalyst **1** (black circles) was attached to the electrode via π- π stacking interactions. Further activation of the precatalyst led to the formation of the final photoanode "Si/TiO_2/C/CNT/[**1**+**1(O)**]".

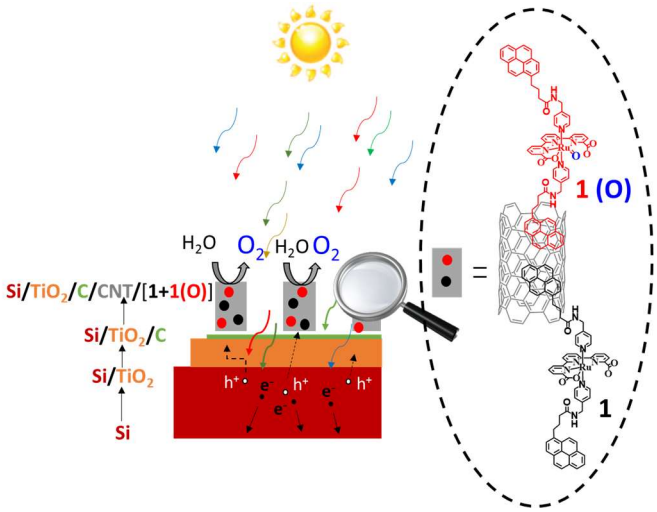

We report herein a hybrid molecular photoanode synthesized by coupling the molecular water oxidation precatalyst $[Ru^{IV}(tda)(py\text{-}pyr)_2(O)]$, **1(O)**, ($tda^{2-}$ is [2,2':6',2''-terpyridine]-6,6''-dicarboxylato; py-pyr is 4-(pyren-1-yl)-N-(pyridin-4-ylmethyl)butanamide) (Scheme I) to a protected Si semiconductor photoelectrode. In molecular form, complex **1(O)** exhibits maximum turnover frequency of > 7700 s^{-1} at pH = 7 (η > 600 mV) for water oxidation to O_2(g), and is generated from the precursor complex $[Ru^{II}(tda)(py\text{-}pyr)_2]$, **1**.

Scheme I describes the preparation of the hybrid Si photoanodes. Phosphorous doped n-Si wafers were used to assess the performance of the electrodes under illumination, whereas highly boron-doped p^+-Si electrodes were used to assess the electrochemical properties of Si-based electrodes in the dark. The Si substrates were coated with 60 nm of amorphous TiO_2 produced by atomic-layer deposition (ALD).[15] 20 mm of graphitic carbon was sputtered onto the TiO_2 to avoid deleterious effects associated with the resistance of the top-most TiO_2 layer.[15] A thick layer of multi-walled carbon nanotubes (CNT) was then drop cast over the Si/TiO_2/C substrate.[9] A layer of poly(methyl methacrylate) (PMMA) was drop cast on top of the CNT, to enhance the mechanical stability of whole assembly, producing a material that is designated herein as Si/TiO_2/C/CNT. The CNT layer was 14 ± 1 μm thick, as evidenced by scanning-electron microscopy (SEM) (Figure S2). A pattern of holes was then scratched on top of the CNT to improve the light absorptivity by the Si in the presence of the thick overlayer of black CNT. The Si/TiO_2/C/CNT substrates were then soaked for 12 h in a solution of complex **1,** to immobilize the complex on the CNT layer and to generate the Si/TiO_2/C/CNT/**1** substrates (see Supporting Information for experimental details).

Figure 1A shows the CVs for p^+-Si/TiO_2/C/CNT/**1** and n-Si/TiO_2/C/CNT/**1** electrodes at pH = 7.0 in the dark and under 3 Sun illumination, respectively. The voltammetry exhibited two reversible waves that shifted by -240 mV between the p^+-Si and n-Si electrodes, consistent with the measured V_{oc} in contact with $[Fe(CN)_6]^{3-/4-}$(aq) (see Figure S4 for the $[Fe(CN)_6]^{3-/4-}$ data). The two redox waves are consistent with the III/II and IV/III redox couples of complex **1** anchored at the photoanode. The midpoints of the redox waves on molecularly functionalized p^+-Si surfaces were at nearly identical potentials to those exhibited by **1** in homogeneous solution using glassy carbon as a working electrode.[3] Integration of the charge under the waves yielded a coverage of 14.6 ± 2.4 nmol cm^{-2} and 13.0 ± 2.2 nmol cm^{-2} for p^+-Si and n-Si electrodes, respectively (Figure S6; Table S1). The amount of **1** on the surface and its size suggests that the surface of the CNTs was near fully covered. The increase in current density at potentials > 1.3 V vs the normal hydrogen electrode, NHE, is consistent with oxidation of the CNT.[9] All potentials reported herein are referenced to NHE.

To generate the water oxidation precatalyst **1(O)** at the surface, the surface-bound complex **1** was electrochemically oxidized from the II to the IV oxidation state, and held at an oxidizing potential to allow partial incorporation of an aqua ligand into the coordination sphere (eqs 1, 2).[3,9] Accordingly, p^+-Si/TiO_2/C/CNT/**1** electrodes were subjected to chronoamperometry (CA) for 150 s at E = 1.30 V in the dark, whereas n-Si/TiO_2/C/CNT/**1** electrodes were maintained for 150 s at E = 1.10 V under 3 Sun illumination. The resulting electrodes were rinsed with water and introduced into a fresh solution at pH = 7.

$$Si/TiO_2/C/CNT/\mathbf{1} - 2e^- \rightarrow Si/TiO_2/C/CNT/\mathbf{1}^{2+} \quad (1)$$

$$Si/TiO_2/C/CNT/\mathbf{1}^{2+} + OH^- \rightleftharpoons Si/TiO_2/C/CNT/[\mathbf{1(O)}] + H^+ \quad (2)$$

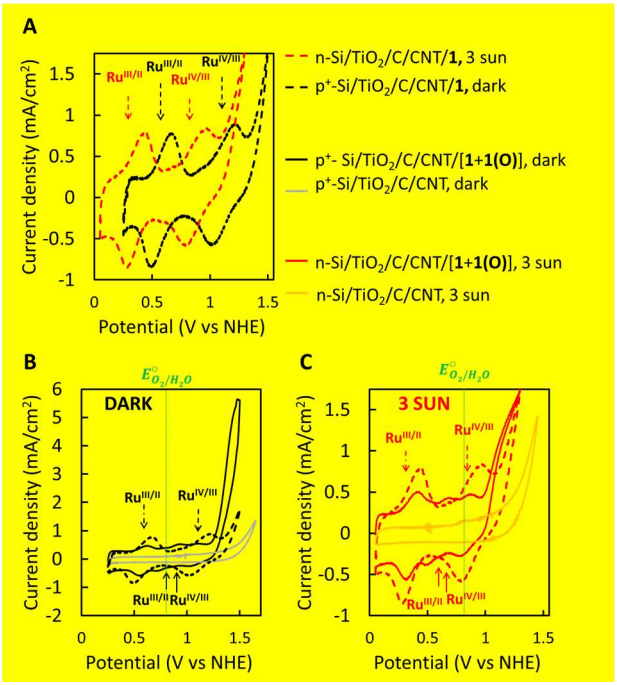

Figure 1. **A**, CV of p⁺-Si/TiO_2/C/CNT/**1** in the dark (black dashed line) and n-Si/TiO_2/C/CNT/**1** (red dashed line) under 3 sun illumination at pH = 7 together with the assignment of the redox processes shown in dashed black and red arrows, respectively. **B**, CV of p⁺-Si/TiO_2/C/CNT/**1** (black dashed line), p⁺-Si/TiO_2/C/CNT/[**1**+**1(O)**] (black solid line) and as prepared bare p⁺-Si/TiO_2/C/CNT electrode (grey solid line) in the absence of illumination at pH = 7, together with the assignment of the redox processes of complex **1** and complex **1(O)** indicated with dashed and black arrows, respectively. **C**, CV of n-Si/TiO_2/C/CNT/**1** (red dashed line), n-Si/TiO_2/C/CNT/[**1**+**1(O)**] (red solid line) and as prepared bare n-Si/TiO_2/C/CNT electrode (orange solid line) under 3 sun illumination at pH = 7 together with the assignment of the redox processes of complex **1** and complex **1(O)** indicated with dashed and solid red arrows, respectively.

Figures 1B and 1C show the cyclic voltammetry of the activated precatalyst on n-Si/TiO_2/C/CNT/[**1**+**1(O)**] and p⁺-Si/TiO_2/C/CNT/[**1**+**1(O)**] electrodes with and without illumination, respectively. Figure 1B shows the CV behavior of a p⁺-Si/TiO_2/C/CNT/[**1**+**1(O)**] electrode as well as p⁺-Si/TiO_2/C/CNT/**1** and a bare p⁺-Si/TiO_2/C/CNT electrode. The appearance of waves ascribable to **1(O)** in the 0.65 to 0.96 V region was accompanied by the growth of catalytic current in the 1.20 to 1.45 V potential range. Similar behavior was observed in the voltammetry of n-Si/TiO_2/C/CNT/**1** and n-Si/TiO_2/C/CNT/[**1**+**1(O)**] electrodes under 3 Sun illumination at pH = 7 (Figure 1C), with the expected with the expected -240 mV potential shift relative to the analogous p⁺-Si electrode. The magnitude of the voltammetric peaks in the 0.4 to 0.7 V region correlated with the increase in current density in the 1.0 to 1.30 V region associated with electrocatalytic oxidation of water to dioxygen. The n-Si electrodes under 3 Sun illumination exhibited sigmoidal catalytic current at positive potentials (Figure 1C). Figure 2A shows the voltammetry of n-Si/TiO_2/C/CNT/[**1**+**1(O)**] electrodes under 1, 2 and 3 sun illumination, respectively, clearly indicating the sigmoidal behavior of the catalytic response under these conditions and consistent with the light-limiting current density in the $Fe(CN)_6]^{4-/3-}$ measurements (Figure S4).

Figures 1B and 1C show the cyclic voltammetry of the activated precatalyst on n-Si/TiO_2/C/CNT/[**1**+**1(O)**] and p⁺-Si/TiO_2/C/CNT/[**1**+**1(O)**] electrodes with and without illumination, respectively. Figure 2B shows chronopotentiometry at 1 mA cm^{-2} for a p⁺-Si/TiO_2/C/CNT/[**1**+**1(O)**] electrode and for a bare p⁺-Si/TiO_2/CNT electrode, respectively, while the amount of oxygen generated was measured with a Clark electrode in the headspace of the electrochemical cell. Faradaic efficiencies for O_2(g) evolution were >90% for the p⁺-Si/TiO_2/C/CNT/[**1**+**1(O)**] electrodes. Similar Faradaic efficiencies were obtained for the related catalyst in solution[3] or for **1(O)** immobilized on CNT.[9] The Faradaic efficiency for O_2(g) production was ~5% for the bare p⁺-Si/TiO_2/C/CNT electrode (Figure S7).

An analogous chronopotentiomety experiment was performed for n-Si/TiO_2/C/CNT/[**1**+**1(O)**] electrodes in the presence of 1, 2 or 3 Sun illumination, respectively (Figure 2C). The observed shifts in potential are in accord with the negative shift in potential provided by the photoelectrode relative to the p⁺-Si electrode. At longer times, the three electrodes exhibited an increase in potential regardless of the light intensity.

After O_2 evolution, the voltammetry indicated that the catalytic activity and the precatalyst loading decreased by 30–50% relative to their initial values, but no new electroactive species were detected in the voltammetry (Figure S8). This behavior is consistent with the partial loss of CNT-Ru material from the electrode. A positive shift in potential was observed during a 3 h chronopotentiometric experiment at $J = 1$ mA cm^{-2} for n-Si/TiO_2/C/CNT/[**1**+**1(O)**] under 3 Sun illumination at pH = 7, consistent with a decrease of the catalytic activity correlated with the decrease in the amount of precatalyst on the photoanode as monitored by cyclic voltammetry (see Figure S9). Assuming that the O_2(g) evolution arose solely from the **1(O)** molecular species implies a TON of ~6.0×10^4 for the n-Si/TiO_2/C/CNT/[**1**+**1(O)**] photoanode (Table S3-S4). Formation of trace amounts of RuO_2 as the actual catalytic species in the activation procedure or during catalysis cannot be ruled out from the available data. For comparison, dye-sensitized photoanode systems in which a chromophore, typically a $[Ru(bpy)_3]^{2+}$-type of complex modified with a phosphonic acid functionalization, and a water-oxidation catalyst modified in a similar manner, are assembled at the surface of a large band-gap metal oxide semiconductor, such as TiO_2,[16] yield current densities of 1 mA cm^{-2} for < 20 min of O_2(g) evolution at 0.3 V vs NHE at pH ~ 6.[10,11]

The hybrid molecular photoanode described herein provides facile anchoring of the precatalyst through the pyrene group. The present Si/TiO_2/C configuration allows evaluation of the electrochemical features of the precatalyst over a large potential window, in contrast to wide band-gap oxide based semiconductors (e.g WO_3, $BiVO_4$) which often mask the electroactivity of the catalyst at very positive potentials. The cyclic voltammetric behavior of Si/TiO_2/C/CNT/[**1**+**1(O)**] allows evaluation of the loading, nature of the bound complexes, and stability of the complex during and after the catalysis.[6] The high stability of the π–π bond between the pyrene functionality of the water oxidation precatalyst and the CNT contrasts with the limited stability of a M-OP bond for binding either chromophores or catalysts in the dye-sensitized solar cell configurations, due to the competing effect of the buffer solutions for the same surface bond. [12] The simplicity of the precatalyst anchoring process may facilitate extension of the approach to applications such as the light-induced transformation of organic substrates.[17]

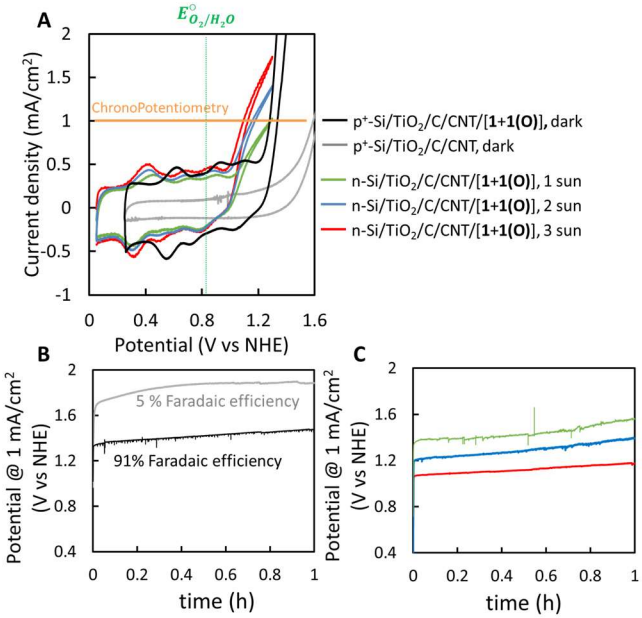

Figure 2. **A**, CV of the n-Si/TiO_2/C/CNT/[**1**+**1(O)**] electrodes at pH = 7 under 1, 2 and 3 sun illumination (green, blue and red lines), respectively, together with the cyclic voltammetry of p^+-Si/TiO_2/C/CNT/[**1**+**1(O)**] (black line) and as prepared bare p^+-Si/TiO_2/C/CNT (grey line) electrodes at pH = 7 in the dark. **B**, chronopotentiometry at 1 mA cm^{-2} for p^+ electrodes at pH = 7 in the dark. **C**, CP at 1 mA cm^{-2} for n electrodes under 1, 2 and 3 Sun (green, blue and red lines), respectively.

The low-energy pathway associated with catalysis effected by **1(O)** is believed to involve a water nucleophilic attack mechanism, WNA,[2,3] which is compatible with the restricted mobility conditions produced when the catalyst is anchored on a photoanode.[9] This putative mechanism is consistent with the observed increase in stability of the photoanode described herein as compared to electrodes that use a Ru-bda (bda is 2,2'-bipyridine-6,6'dicarboxylate) moiety, whose low-energy water-oxidation pathway is believed to involve a metal-based bimolecular mechanism, I2M, ultimately leading directly to decomposition to RuO_2.[6]

The light-induced water oxidation potential ranged from 1.2 to 1.4 V, whereas the potential of the top of the Si valence band is ~ 1 V vs NHE.[18] The Si/TiO_2/C configuration is a buried junction device that outputs a photovoltage, so the positions of the band edge of the Si are not important. This is advantageous relative to a dye-sensitized solar cell in which water oxidation will occur only at potentials more negative than those of the Ru(III)/Ru(II) couple in the $[Ru(bpy)_3]^{2+}$-type of dye used as the light absorber. Further performance improvements can certainly be obtained, because Si/TiO_2 photoanodes in 1.0 KOH(aq) with Ni-oxyhydroxide heterogeneous OER catalysts exhibit V_{oc} >0.5 V and J_{sc} >20 mA cm^{-2} under analogous test conditions.[15]

An important limitation of the n-Si photoanodes investigated herein is the reduced amount of light absorption by the Si due to absorption by the relatively thick CNT layer that covers ~80% of the surface. Small but non-zero oxidation of the CNT support, presumably correlated with the deanchoring process, also occurs in parallel with water oxidation and would reduce the faradaic efficiency at very positive potentials. The latter desorption can in principle be overcome by the use of water oxidation catalysts that operate at lower overpotentials, as such species are developed.

In conclusion, a hybrid photoanode based on a molecular Ru complex attached via π-staking on CNTs previously deposited on a TiO_2-coated Si semiconductor can effect the oxidation of water to O_2(g) with high faradaic efficiency. The Ru based hybrid photoanode is stable for over 60 min of operation at current densities of 1 mA cm^{-2} while maintaining intact the molecular precatalyst. The Si/TiO_2/C configuration permits facile anchoring of a molecular precatalyst previously functionalized with extended π-systems and facilitates monitoring of the nature of the molecular species on the photoanode before and during catalysis.

AUTHOR INFORMATION

Corresponding Authors. allobet@iciq.es; nslewis@caltech.edu

ASSOCIATED CONTENT

Supporting information. Experimental section, additional characterization and electrochemical data. This material is available free of charge via the Internet at http://pubs.acs.org.

AKNOWLEDGEMENTS

The National Science Foundation under NSF Center CHE-1305124 provided support for H.B.G., I.M.H, N.S.L., B.S.B. and R.M and for supplies at Caltech, I.M.H. was supported by a NSF Graduate Research Fellowship (Grant No. DGE-1144469). Instrumentation support was also provided by the Molecular Materials Resource Center of the Beckman Institute at California Institute of Technology. R.M., A.L. and X.S. acknowledge MINECO and FEDER (CTQ2016-80058-R, CTQ2015-64261-R, SEV 2013-0319, ENE2016-82025-REDT, CTQ2016-81923-REDC), AGAUR (2014-SGR-915) and "La Caixa" foundation. We acknowledge Dr. K. Sun for helpful discussions.

REFERENCES

(1)McCrory, C. C. L.; Jung, S.; Ferrer, I. M.; Chatman, S. M.; Peters, J. C.; Jaramillo, T. F. *J. Am. Chem. Soc.* **2015**, *137*, 4347-4357
(2)Concepcion, J. J.; Tsai, M. K.; Muckerman, J. T.; Meyer, T. J. *J. Am. Chem. Soc.* **2010**, *132*, 1545-1557.
(3)Matheu, R.; Ertem, M. Z.; Benet-Buchholz, J.; Coronado, E.; Batista, V. S.; Sala, X.; Llobet, A. *J. Am. Chem. Soc.* **2015**, *137*, 10786-10795.
(4)Duan, L.; Bozoglian, F.; Mandal, S.; Stewart, B.; Privalov, T.; Llobet, A.; Sun, L. *Nat. Chem.* **2012**, *4*, 418-423.
(5)Moonshiram, D.; Pineda-Galvan, Y.; Erdman, D.; Palenik, M.; Zong, R.; Thummel, R.; Pushkar, Y. *J. Am. Chem. Soc.* **2016**, *138*, 15605-15616.
(6)Matheu, R.; Francàs, L.; Chernev, P.; Ertem, M. Z.; Batista, V.; Haumann, M.; Sala, X.; Llobet, A. *ACS Catal.* **2015**, *5*, 3422-3429.
(7)Brennaman, M. K.; Dillon, R. J.; Alibabaei, L.; Gish, M. K.; Dares, C. J.; Ashford, D. L.; House, R. L.; Meyer, G. J.; Papanikolas, J. M.; Meyer, T. J. *J. Am. Chem. Soc.* **2016**, *138*, 13085-13102.
(8)Chen, Z.; Concepcion, J. J.; Jurss, J. W.; Meyer, T. J. *J. Am. Chem. Soc* **2009**, *131*, 15580-15581.
(9)Creus, J.; Matheu, R.; Peñafiel, I.; Moonshiram, D.; Blondeau, P.; Benet-Buchholz, J.; García-Antón, J.; Sala, X.; Godard, C.; Llobet, A. *Angew. Chem. Int. Ed.* **2016**, *55*, 15382-15386.
(10)Gao, Y.; Ding, X.; Liu, J.; Wang, L.; Lu, Z.; Li, L.; Sun, L. *J. Am. Chem. Soc.* **2013**, *135*, 4219-4222.
(11) (a) Sheridan, M. V.; Sherman, B. D.; Coppo, R. L.; Wang, D.; Marquard, S. L.; Wee, K.-R.; Murakami Iha, N. Y.; Meyer, T. J. *ACS Energy Lett.* **2016**, *1*, 231-236. (b) Sheridan, M. V.; Hill, D. J.; Sherman, B. D.; Wang, D.; Marquard, S. L.; Wee, K.-R.; Cahoon, J. F.; Meyer, T. J. *Nano Letters* **2017**, *17*, 2440-2446.
(12)Hyde, J. T.; Hanson, K.; Vannucci, A. K.; Lapides, A. M.; Alibabaei, L.; Norris, M. R.; Meyer, T. J.; Harrison, D. P. *ACS App. Mat. Inter.* **2015**, *7*, 9554-9562
(13)Wee, K.-R.; Brennaman, M. K.; Alibabaei, L.; Farnum, B. H.;

Sherman, B.; Lapides, A. M.; Meyer, T. J. *J. Am. Chem. Soc.* **2014**, *136*, 13514-13517.
(14)Zhou, X.; Liu, R.; Sun, K.; Papadantonakis, K. M.; Brunschwig, B. S.; Lewis, N. S. *Energy Environ. Sci.* **2016**, *9*, 892.
(15)Hu, S.; Shaner, M. R.; Beardslee, J. A.; Lichterman, M.; Brunschwig, B. S.; Lewis, N. S. *Science* **2014**, *344*, 1005-1009.
(16)Gratzel, M. *Acc. Chem. Res.* **2009**, *42*, 1788-1798.
(17)Farras, P.; Di Giovanni, C.; Clifford, J. N.; Garrido-Barros, P.; Palomares, E.; Llobet, A. *Green Chem.* **2016**, *18*, 255-260.
(18)Plymale, N. T.; Ramachandran, A. A.; Lim, A.; Brunschwig, B. S.; Lewis, N. S. *J. Phys. Chem. C* **2016**, *120*, 14157-14169.

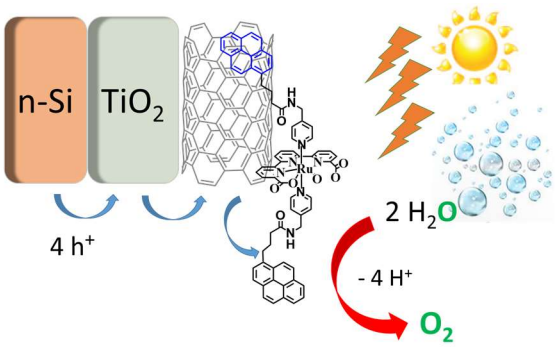
n-Si
TiO2
4 h+
2 H2O
- 4 H+
O2